Theoretical & Applied Mechanics Letters 7 (2017) 181–184

Contents lists available at ScienceDirect

Theoretical & Applied Mechanics Letters

journal homepage: www.elsevier.com/locate/taml

Letter

Passive control of cavitating flow around an axisymmetric projectile by using a trip bar

Jian Huang [a], Chao Yu [a,b], Yiwei Wang [a,b,*], Chang Xu [a], Chenguang Huang [a,b]

[a] *Key Laboratory for Mechanics in Fluid Solid Coupling Systems, Institute of Mechanics, Chinese Academy of Sciences, Beijing 100190, China*
[b] *School of Engineering Science, Institute of Mechanics, Chinese Academy of Sciences, Beijing 100049, China*

HIGHLIGHTS

- It's useful to control the cavitating flow by adding a trip bar on the axisymmetric projectile.
- The re-entrant jet and collapse pressure are obstructed and weakened.
- Isolation system is formed upstream of the bar.

ARTICLE INFO

Article history:
Received 20 April 2017
Received in revised form 6 August 2017
Accepted 22 August 2017
Available online 27 September 2017
*This article belongs to the Fluid Mechanics.

Keywords:
Unsteady cavitating flow
Trip bar
Re-entrant jet
Passive flow control

ABSTRACT

Quasi-periodical evolutions such as shedding and collapsing of unsteady cloud cavitating flow, induce strong pressure fluctuations, what may deteriorate maneuvering stability and corrode surfaces of underwater vehicles. This paper analyzed effects on cavitation stability of a trip bar arranged on high-speed underwater projectile. Small scale water tank experiment and large eddy simulation using the open source software OpenFOAM were used, and the results agree well with each other. Results also indicate that trip bar can obstruct downstream re-entrant jet and pressure wave propagation caused by collapse, resulting in a relatively stable sheet cavity between trip bar and shoulder of projectiles.

Cavitation occurs in low-pressure regions on surfaces of high-speed underwater vehicles. Unsteady evolutions, such as shedding and collapsing of cavity, can lead to negative influences, including vibration, noise, and cavitation erosion, on underwater vehicles. Consequently, effective flow control methods must be designed to improve stability of cavitating flow and to ensure safety of high-speed underwater cruising. Previous research showed that re-entrant jet inside cavities is a key factor causing transformation of sheet cavitation to cloud cavitation and eventual cavity collapse [1–3]. Unsteady cavity evolution can also be affected by pressure wave caused by collapsing [4–6].

Two main kinds of cavitating flow control methods are available. Active controls commonly realized by ventilation. Cavity shedding and collapsing are suppressed, and when flow pattern changes from bubble-layer to air-layer with increasing gas-injection mass flux, sailing resistance can be decreased simultaneously [7]. However, difficultly arises from achieving such process. By contrast, passive control is easier to implement. Attaching a trip bar on the upper surface of a NACA16012 hydrofoil can change boundary layer and local flow characteristics, suppressing the unsteady evolution of cavity flow [8]. Further studies must be conducted for adjustments for other geometric shapes of underwater vehicle.

For cavitation of axisymmetric projectiles, shedding and collapsing induced by re-entrant jet become more significant. Re-entrant jet is generated at the trailing edge of cavity then moves to the leading edge along projectile surface and finally cuts off cavitation that leads to shedding and collapse. Collapse pressure possibly further strengthens re-entrant jet in the next cycle [9]. Evolutionary characteristics of axisymmetric projectile cavitation are similar to those of hydrofoil cavitation. Consequently, the trip bar may improve cavitation stability by weakening re-entrant jet. Thus far, no work discussed this subject.

In this paper, typical experiments of unsteady cavitating flow around axisymmetric projectiles were carried out by using the Split-Hopkinson pressure bar (SHPB) launch system in an open water tank. Experimental results were compared with numerical

* Corresponding author at: Key Laboratory for Mechanics in Fluid Solid Coupling Systems, Institute of Mechanics, Chinese Academy of Sciences, Beijing 100190, China.
E-mail address: wangyw@imech.ac.cn (Y. Wang).

https://doi.org/10.1016/j.taml.2017.09.003
2095-0349/

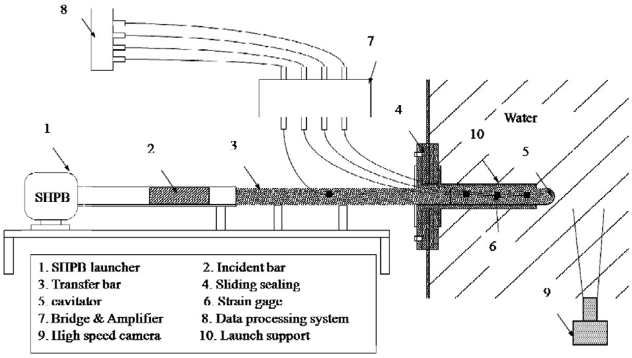

Fig. 1. Test principle and system components.

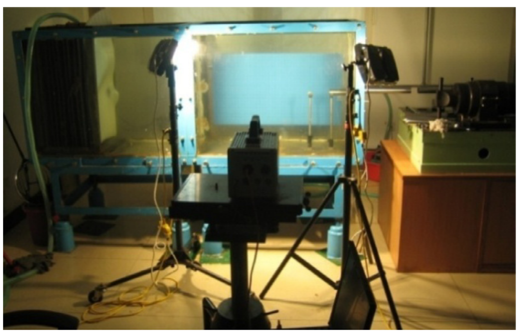

Fig. 2. The photo of experimental facility.

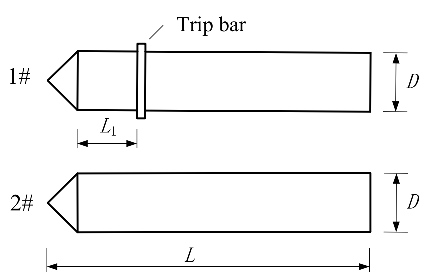

Fig. 3. Designs of test models: with the trip bar (1#) & without the trip bar (2#).

simulations that are based on open source computational fluid dynamics code OpenFOAM. Influence of trip bar on stability of cavities was studied by comparing cavitation evolutions and flow patterns with and without the bar.

The experimental facility consisted of SHPB launch system, an open water tank, and a high-speed camera. Test principle and system components are shown in Fig. 1, and photo of the device is presented in Fig. 2. Specific description of the facility was introduced in Ref. [10]. Projectile can be transiently accelerated to 30 m/s in less than 50 μs. Through images of cavitation evolution, processes were recorded by high-speed photography with sampling frequency of 20 000 frames per second.

Total length of test models (L) measures 200 mm; diameter (D) is 37 mm; and cone angle of conical head is 90° (as shown in Fig. 3). Among these models, a trip bar is set on model 1# with a 5 mm × 5 mm rectangular cross-section. Distance from shoulder of projectile (L_1) to the bar equals the diameter; model 2# is set without the bar as contrast.

During experiments, environment temperature was 25 °C. The main air chamber pressure of launching system measured 1.0 Mpa when the two models were launched. Initial speeds of models were

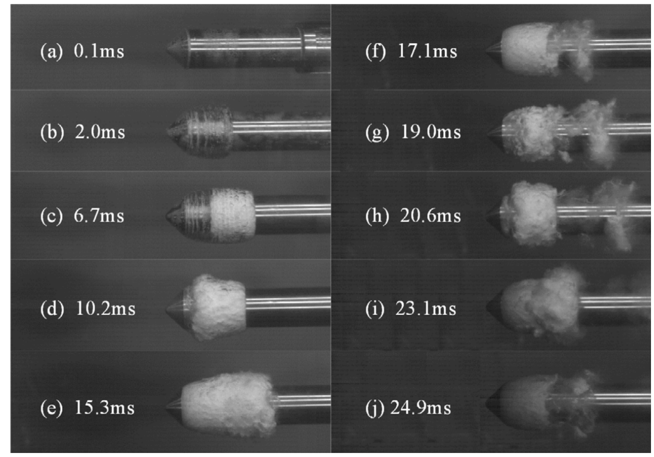

Fig. 4. The cavitation evolution of the projectile without a bar.

obtained by image analysis. Speed of model1# measured 21.4 m/s, and that of model 2# reached 21.2 m/s.

Cavitation evolution of axisymmetric projectile includes growth, shedding, and collapse. Re-entry jet is often considered the primary cause of cavity shedding. Figure 4 shows processes of main cavitation evolution of projectile without the bar. Figure 4(a–c) present cavity growth. Re-entrant jet was already generated and moved to the middle of cavity along the projectile surface. Cavity shed from the leading edge to downstream, then collapsed near the trailing edge of the main cavity, as shown in Fig. 4(d–g). Collapse pressure spread upstream and reinforced re-entrant jet by increasing adverse pressure gradient, as shown in Fig. 4(g). New re-entrant jet then caused shedding and collapsing in the next period (as shown in Fig. 4(h–j)).

Cavitation evolution features different processes after adding the bar, as shown in Fig. 5. Cavity growth is shown in Fig. 5(a–c). Cavitation occurred around both shoulder and the bar; this cavitation is the main difference compared with the case without the bar. First cavity collapse is shown in Fig. 5(f–h). Cavity behind the bar cracked when shedding from shoulder cavity crossed the bar, as shown in Fig. 5(f). The latter cavity then collapsed in less than one millisecond, as shown in Fig. 5(g). Figure 5(h) shows that re-entrant jet was blocked by the bar. Weakened re-entrant jet then transferred to projectile shoulder and caused shedding and collapse in the next period, as shown in Fig. 5(i–k) and (l–n).

Variations in cavity length and thickness (as shown in Fig. 6) were also compared. The cavity sizes were obtained by conversing based on pixels. The measurement error might be no more than 1 pixel, about 0.5 mm. Cavity length L_c was measured from projectile shoulder to end of cavity. Cavity thickness was measured from projectile surface to outermost cavity surface. During observation, variations and thickness in cavity length were compared between cases with and without the trip bar, as shown in Fig. 7.

Cavitation evolution can be illustrated by typical observation time by cavity length variation. Sudden decrease in length represents cavity collapse. The case with the bar showed three collapses, as marked by red arrows in Fig. 7. Two collapses were observed in the case without a bar and were marked by yellow arrows. Variation in cavity thickness is similar to that of length. After adding the bar, maximum length and thickness of cavities reduced slightly; cavity length remained stable for a longer period between two collapses and is shown as the overlap of length curve and dotted line in Fig. 7.

To obtain more detailed information on flow field, numerical simulations were carried out by using OpenFOAM. Large eddy

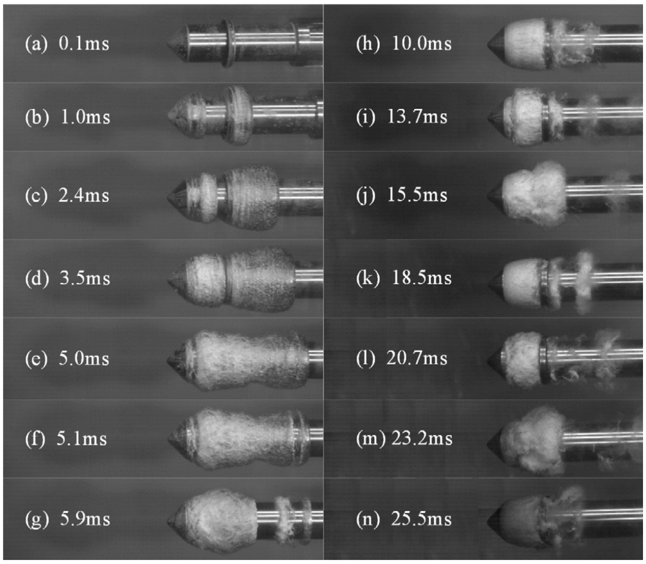

Fig. 5. The cavitation evolution of the projectile with a bar.

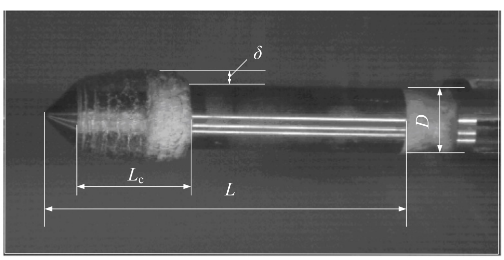

Fig. 6. The diagram of the cavity length and thickness.

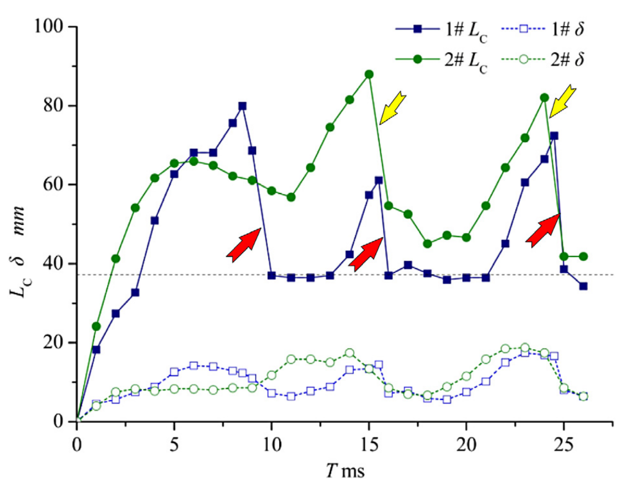

Fig. 7. The variations of cavity length and thickness. (The arrows indicate positions of the cavity collapse, and the horizontal dotted line shows the distance L_1 between the projectile shoulder and the bar.) (For interpretation of the references to colour in this figure legend, the reader is referred to the web version of this article.)

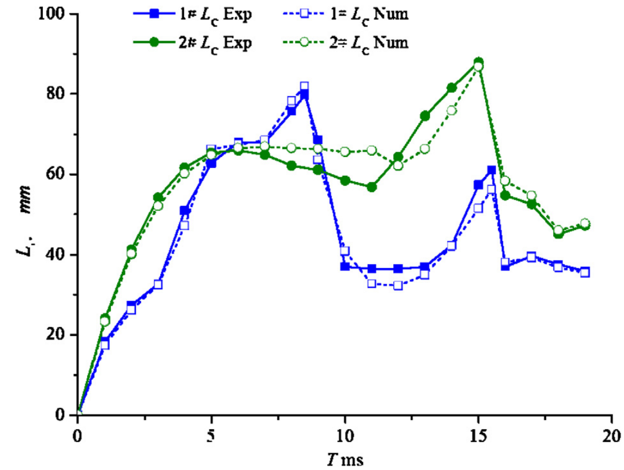

Fig. 8. The comparison of experiment and numerical simulation. (The solid lines represent the cavity lengths in the experiment; the dotted lines represent the cavity lengths in the numerical simulation.)

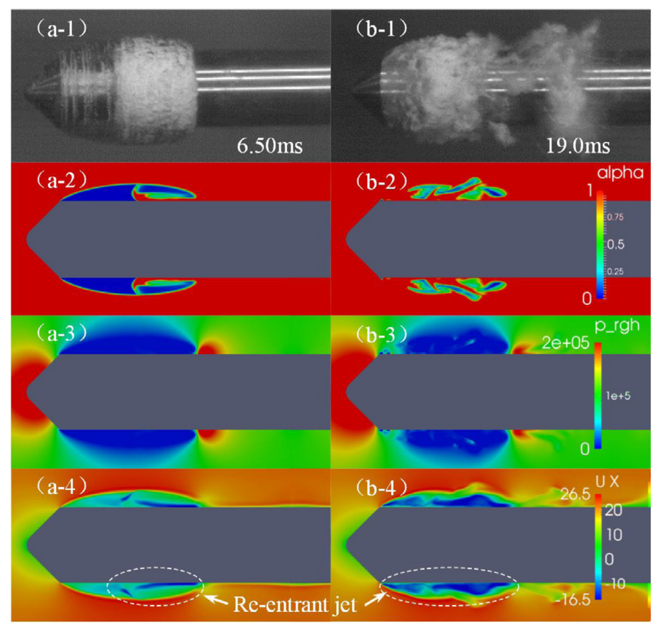

Fig. 9. Shedding and collapse induced by the re-entrant jet without the trip bar. (The first row: the experiment photograph; the second line: the simulation results of the bubble shape, color contour is represented by the volume fraction of liquid water; the third line: the simulation results of the bubble pressure field, color contour is represented by the pressure of water or vapor; the fourth line: the simulation results of the velocity field along the flow direction, color contour is represented by the speed of water along the length of projectile.) (For interpretation of the references to colour in this figure legend, the reader is referred to the web version of this article.)

simulation (LES) method, volume of fluid multiphase flow, and Kunz cavitation models were adopted. Governing equations are quoted in Ref. [11]. In Fig. 8, the cavity lengths from numerical simulation were agree well with the experiment. Furthermore, cavity shapes that were obtained from numerical simulations approximately coincided with corresponding experimental results at typical moments, as shown in the first two rows of Figs. 9 and 10. Both of them indicated reliability of numerical simulations.

We focused on mechanism of bar effects on re-entrant jets, which started during the last cycle of cavitation shedding and ended while arriving at the shoulder of projectiles. Consequently, for the case without the bar, cavities at 6.5 and 19.0 ms were selected. Figure 9 shows experimental and numerical simulation results. For projectile with the bar, selected moments of movement of re-entrant jet measured 9.6 and 13.0 ms before and after the bar, respectively, as shown in Fig. 10.

Figure 9(a) shows that the re-entrant jet moved along projectile surface toward the shoulder in the first period. With generated projectile)

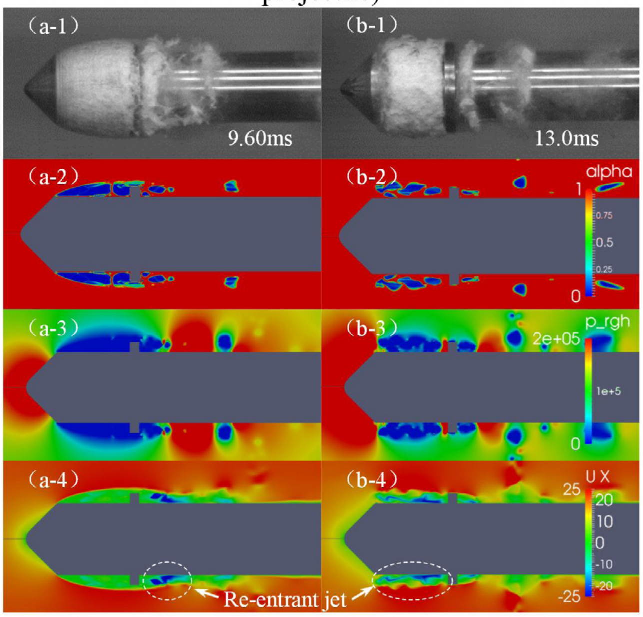

Fig. 10. Influence of the trip bar on the cavitation evolution.

adverse pressure gradient at trailing edge of cavity and without the blocking effect of the bar, the re-entrant jet moved to the shoulder with little resistance, causing large-scale shedding. Shedding then drifted to down flow and eventually collapsed. Figure 9(b) shows complete crashing of cavity, and propagation of collapse pressure wave caused disorder in cavity interface and strengthened the re-entrant jet by enhancing pressure at end of cavity.

After adding the trip bar, collapse pressure and re-entrant jet crossed it to reach the leading edge of cavity as collapse occurred downstream of the bar. Figure 10(a) shows collapse that occurred downstream of the bar, whereas Fig. 10(b) shows cavity shape prior to next shedding. As shown in Fig. 10(a-1 and a-2), upstream cavity of the bar remained relatively smooth. Figure 10(a-3) shows that high pressure of collapse occurred downstream. Collapse-enhanced re-entrant jet was prevented by the trip bar when it spread upstream. Figure 10(a-4) shows that resistance of the bar to re-entrant jet induced by collapse. Figure 10(b) shows that at this point, new cavitation shedding occurred. Based on velocity field in Fig. 4(b), the re-entrant jet caused collapse that initiated upstream of the bar, whereas Fig. 10(b-3) shows the re-entrant jet driven by high pressure on upstream side of the bar. Conditions were different without the bar, and the main cause for re-entrant jet was collapse pressure at cavity end. Therefore, as shown in the overall analysis in Fig. 10, the bar isolated front and rear regions into two approximately independent systems. Re-entrant and shedding occurred upper-stream of the bar. However, collapse transpired downstream. Thus, the bar inhibited adverse effects of collapse on cavitation stability.

As a result of inhibition to collapse pressure and re-entrant after adding the trip bar, cavitation stability was effectively promoted. Stable cavity is one of the features that exists between the bar and projectile shoulder for long periods. Figure 7 shows that cavity length maintained a stable length in nearly half a cycle of time between two adjacent collapses. For example, the steady state (16–21 ms) in the third cycle were shown in Fig. 5(k) and (l). If there was no trip bar, the cavity would experience a completely collapse, as shown in Fig. 4(g). So cavitation stability can be improved by the trip bar.

In summary, through analysis of experimental and simulated results, the following conclusions are obtained: In unsteady evolution of cavitation, the trip bar can effectively weaken re-entrant jet and block propagation of pressure wave caused by collapse. Isolation system is formed upstream of the bar where stable cavity is present as shock induced by collapse can be weakened significantly. The next study will focus on the optimization of the bar geometry and location, to further improve the stability of the cavity.

Acknowledgments

The authors are grateful to the National Nature Science Foundation of China (11332011 and 11202215).

References

[1] C.E. Brennen, Cavitation and Bubble Dynamics, Oxford University Press, USA, 1995.
[2] B. Stutz, S. Legoupil, X-ray measurements within unsteady cavitation, Exp. Fluids 35 (2) (2003) 130–138.
[3] M. Callenaere, J.P. Franc, J. Michel, et al., The cavitation instability induced by the development of a re-entrant jet, J. Fluid Mech. 444 (2001) 223–256.
[4] R.E.A. Arndt, C.C.S. Song, M. Kjieldsen, et al., Instability of partial cavitation-A numerical & experimental approach, in: Symposium on Naval Hydrodynamics, 2011, pp. 599–615.
[5] H. Ganesh, Bubbly Shock Propagation As a Cause of Sheet to Cloud Transition of Partial Cavitation and Stationary Cavitation Bubbles Forming on a Delta Wing Vorte (Ph.D. thesis), University of Michigan, 2015.
[6] Y. Wang, C. Huang, X. Fang, et al., Cloud cavitating flow over a submerged axisymmetric projectile and comparison between 2D RANS and 3D LES methods, ASME J. Fluids Eng. 138 (2016) 061102.
[7] X. Yu, Y. Wang, C. Huang, et al., Parameters and influence of gas injection on modification of cavitation stability, Sci. Sinica Physica Mech. Astron. 45 (2015) 034703 (in Chinese).
[8] W. Gu, Y. He, Flow control on unstable cavitation phenomena, Chin. J. Theor. Appl. Mech. 33 (2001) 19–27 (in Chinese).
[9] Y. Wang, C. Huang, X. Fang, et al., Cloud cavitating flow over a submerged axisymmetric projectile and comparison between two-dimensional RANS and three-dimensional large-eddy simulation methods, ASME J. Fluids Eng. 138 (2016) 061102.
[10] W. Yi-Wei, H. Chen-Guang, D. Te-Zhuan, et al., Shedding phenomenon of ventilated partial cavitation around an underwater projectile, Chin. Phys. Lett. 29 (2012) 014601.
[11] X. Yu, C. Huang, T. Du, et al., Study of characteristics of cloud cavity around axisymmetric projectile by large eddy simulation, J. Fluids Eng. 136 (2014) 051303.